

## Tomographic imaging with a Bonse-Hart camera

W. Treimer<sup>1), 2)</sup>, M. Strobl<sup>1,2)</sup>, A. Hilger<sup>1),2)</sup>, C. Seifert<sup>1)</sup>, U. Feye-Treimer<sup>1)</sup>

<sup>1)</sup>University of Applied Sciences (TFH) Berlin, Fachbereich II, Luxemburger Str.10,

D – 13353 Berlin , Germany

<sup>2)</sup>Hahn-Meitner-Institut, SF1, Glienicker Straße 100, D – 14109 Berlin, Germany

Keywords: Neutron Tomography, Double Crystal Diffractometer, Refraction Contrast, Imaging, Filtered Back Projection

### Abstract

We used a special double crystal diffractometer (DCD) as a tomography apparatus and investigated refraction and small angle scattering as imaging signals. The recorded data from this DCD include much more information about the object than one gets from common absorption tomography. This is due to the additional, simultaneous registration of absorption, refraction and small angle scattering. Refraction data were used to reconstruct the image of samples that showed weak or even no attenuation (absorption) contrast: It was possible to reconstruct images of samples using refraction data only, even in cases in which common techniques failed. Small angle data were used to image different concentrations of 150nm particles carotene in D<sub>2</sub>O. This new imaging signals offers a number of new possibilities in high resolution non destructive testing.

### Theoretical background

The attenuation of a ray that traverses a two dimensional field of matter is described by a two dimensional linear attenuation coefficient  $\mu(x,y)$  and calculated by the well known line integral [1] – [4],

$$I(t) = I_0 \exp \left( - \int_{ray} \mu(x,y) ds \right) \quad (1)$$

along the path of the ray. One projection is the total set of such line integrals covering the whole field. The mathematical solution is to reconstruct the two dimensional function from its projections, well known since the first half of the last century [1]. Conventional computerised tomography (CT) uses once the attenuation of intensity (transmitted or emitted intensity, change of electric fields, resistances, etc.), magnetic fields (nuclear magnetic resonance tomography) and time as imaging signals. But a neutron or x-ray experiences also other interactions such as scattering, depolarisation, change of the phase that also can be used as imaging signals [5].

Concerning Bonse–Hart cameras (double crystal diffractometer) some efforts have already been made to perform radiography (diffraction enhanced imaging; DEI) at first with small angle scattering and ultra small angle scattering instruments (SAS, USAS) [6]–[8]. It was demonstrated that with these methods one can detect structures by using phase contrast, refraction contrast, scattering data and measured magnetic interaction that would not be seen in conventional tomography. Some of these examples, however, did not show a great progress relating to conventional CT, if one compares e.g. the results in [8].

In the case that attenuation fails as imaging signal the function  $\mu(x,y)$  is  $\sim$  zero and  $I(t) = I_0$ . To image a structure other than by absorption and phase contrast one has to take refraction and diffraction as signals. These processes contain information about the structure, and one measures them as a sum of many interactions. The question was, how can this information be transformed into a signal that can be treated as imaging signal for CT.

Refraction and USAS changes the direction of the neutron (or x-ray) and they are measured as a deviation from the incident beam direction: The ray behind a sample will have a final angle of deflection  $\Delta$ , which is the sum of all individual deflections  $\delta_i$  along the path through the sample:

$$\Delta = \sum_{i=1}^n \delta_i \quad (2)$$

A deflection  $\delta_i$  from the preceding direction is only present at the adjacent volumes with different indices of refraction and if  $\bar{k} \cdot \nabla n(x,y) \sim 0$  ( $\bar{k}$  is the neutron wave vector). One can determine  $\nabla n(x,y)$  and by that  $n(x,y)$  by measuring  $\Delta$  of each path (line integral) and varying the orientation  $\theta$  of the sample from  $0^\circ$  to  $180^\circ$ . If  $\bar{k} = (\bar{k}_\parallel, \bar{k}_\perp)$  is represented by a component parallel and perpendicular to  $\nabla n(x,y)$ , and  $\bar{k}_\perp$  is the component of  $\bar{k}$  parallel to  $\nabla n(x,y)$ , then a point  $P_\theta(t)$  of a projection is given by [9]

$$P_\theta(t) = P(t, \theta) = \int_{\text{Path}} \nabla n(x,y) \cdot \bar{k}_\perp \, ds \quad (3)$$

If the incident direction is known,  $\Delta$  and  $P_\theta(t)$  can be determined from the experiment. The reconstruction of  $n = n(x,y)$  from projections can follow the well known mathematical procedures [3],[4].

In the case of small angle scattering the scattering pattern (i.e. the measured intensity distribution) is broadened due to coherent scattering by structures that have sizes of the order of  $\sim 10\text{nm} - 10\mu\text{m}$ . For both scattering effects, refraction and small angle scattering, one can consider the path of a neutron or X-ray through a sample as a straight line, i.e. the volume of interaction does not change due to refraction or small angle scattering. This assumption can be done because the sum of all deviations is small as compared to the divergence of the beam.

## Experiments

We used materials with very low absorption coefficients or – in the case of composites – materials with very low differences of absorption coefficients. However, refraction, small angle scattering or phase shifts depend on the coherent scattering lengths, and are independent of absorption. In order to record refraction, scattering and also magnetic interactions to some extent the double crystal diffractometer (DCD) seems to be the best choice because of its very high angular resolution which can detect tiny beam deviations due to scattering processes in the sample.

For our tomographic investigations, we used the bent crystal type DCD [10], [11] to measure refraction, absorption and (ultra) small angle scattering simultaneously and independently (Fig. 1). However, the pure refraction or USAS data set are completely different from common absorption data, because they must be converted into deviation angles. The deviation for one scan point and for a certain orientation of the sample is different for each orientation (projection) because it depends on the direction of the incoming beam and it has two signs (+, -)

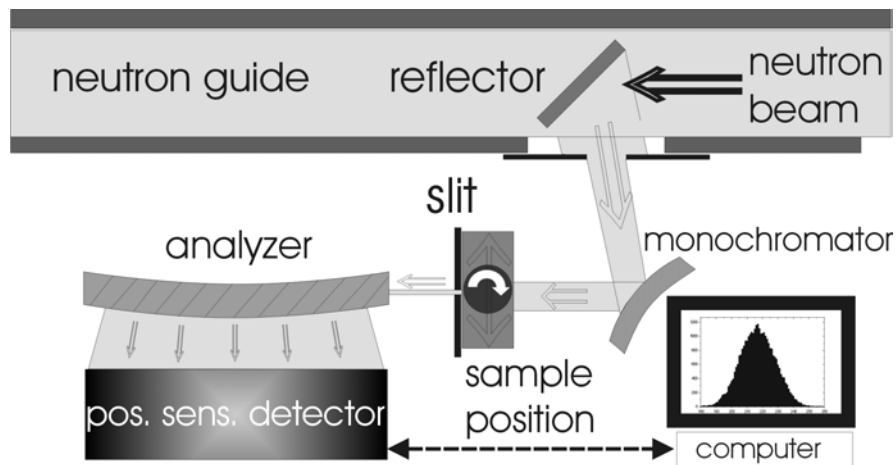


Fig. 1

Double crystal diffractometer V12a at the BER II reactor at the HMI (Berlin)

The symmetric reflecting perfect Si monochromator (111) was bent to a radius of 18,3 m to gain intensity while the asymmetric reflecting analyser (111) was bent to a radius of 47,6 m which provides an angular resolution of 1,4 arcsec per channel at the one dimensional position sensitive detector. The used wavelength was 0.476 nm. Samples to be imaged were positioned on a rotation and translation stage between monochromator and analyser (Fig.1), a slit, quite behind, defined the beam dimensions and determined the spatial resolution of the tomogram, together with the number of projections and exposure time / scan point.

The width of the slit was between 1000  $\mu\text{m}$  and 100  $\mu\text{m}$  for the presented tomographies. The neutron flux at the sample position was  $1.2 \times 10^3$  neutrons /  $\text{cm}^2\text{s}^1$ . The exposure time per shot (scan point) depended on the sample and was 20sec

up to 200sec. Each shot yielded a complete scattering curve over a  $q$  – range of  $2.7 \times 10^{-2} \text{ nm}^{-1}$  registered with 300 channels of a position sensitive detector.

To estimate the sensitivity we calculated the resulting refraction angles for a given sample for one projection and compared the result with experimental data (Fig.2).

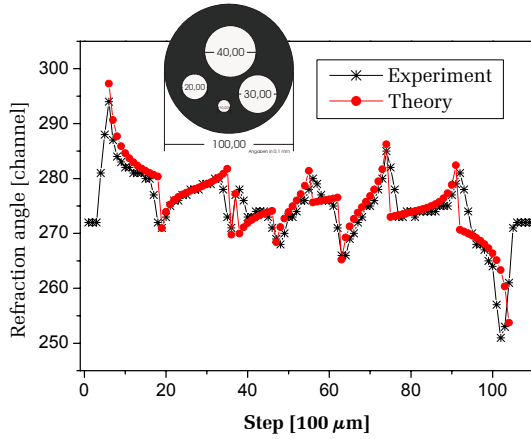


*Fig. 2*  
Calculated and measured beam deviations due to refraction by a sample as shown as insert in the graph, the data were converted into channel numbers of the PSD.

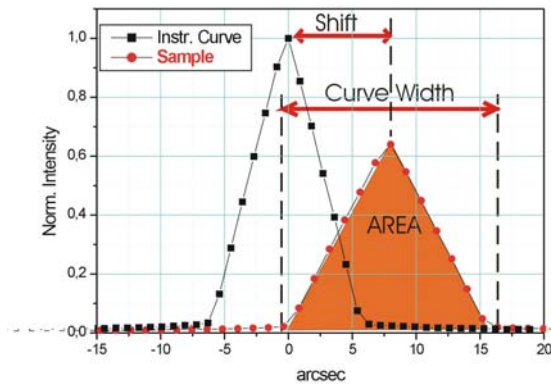
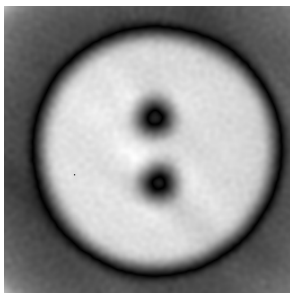
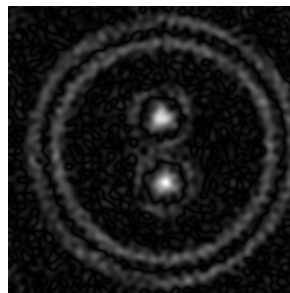


*Fig.3*  
For each scan point, one gets three data for reconstruction

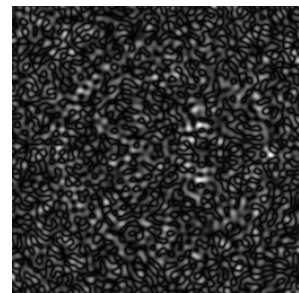
The first sample was an Al cylinder with a diameter of 15 mm and two holes of 2 mm, symmetric to the centre of the cylinder (Fig. 4).



(a)



(b)



(c)

*Fig.4*

*Tomograms (a) and (b) reconstructed (with different methods) from pure refraction data, (c) from absorption data*

The results can be seen to be very satisfying because with the pure refraction signal a clear image could be reconstructed, what could not be realised with absorption data. . Figure 5 shows the tomogram of a brass cylinder with a diameter of 10 mm and holes of 1, 2, 3 and 4 mm diameter (compare insert of Fig. 2). Again, refraction data yielded a much better reconstruction than absorption data did, despite the fact, that brass still an absorbing material.

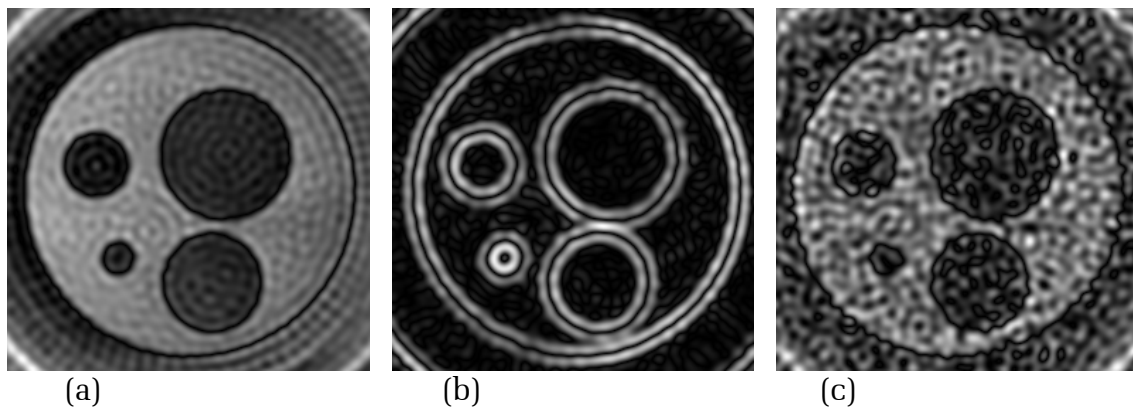


*Fig. 5*

*Tomogram of a brass cylinder,  $\varnothing = 10\text{mm}$ , holes = 1, 2, 3 and 4mm, (a) and (b) reconstruction with refraction data only (different methods), (c) absorption data.*

To be sure that no symmetries or just the simple shape of the structures were responsible for the good reconstruction results a special sample was taken, which got disordered and irregular shapes of holes as can be seen from the reconstruction in Fig.6. Again the sample material was Al and the sample and structure dimensions were enlarged to save beam time by using a large 1 mm slit, keeping in mind, that the dimensions of the structures and also the slit width can be scaled down. The sample was a block of 28 mm x 28 mm and 30mm height, the diameters of the holes were 4 mm and 6 mm diameter and irregular “cuts” in two edges (compare Fig. 6). For each of the 61 projections over  $180^\circ$  the scanning was done by 86 steps with 0.5 mm step width. The smallest Al edges that can also be seen in the reconstruction have a thickness of about 0.4 mm, the exposure time was 30 seconds per step.

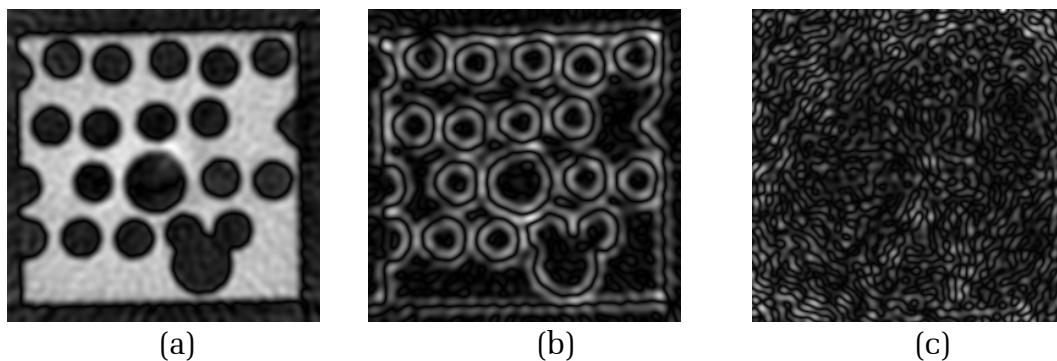


*Fig. 6*

*Tomograms of an Al block, (a) and (b) reconstructions (with different methods) with pure refraction data, (c) absorption data only.*

Small angle scattering data were also used as imaging signals as shown below. Small angle scattering measurements uses thin samples to avoid multiple scattering, what is the case in tomography, where one measures always an integral over a function that has to be reconstructed two-dimensionally. In the case that the particles have different sizes and that they are distributed in a matrix, in a classical small angle scattering experiment one measures a function that consist of the particular scattering patterns from these different particles. A unique spatial and shape distinction is not possible. We found a way to convert SANS data into data that can be used to reconstruct a two-dimensional image of different density concentration of particles distributed in a sample. To distinguish different concentrations we used an Al – Block with several holes and filled them with a liquid sample (solution of  $\beta$ -carotene in  $D_2O$ ) having different concentrations. Fig.7 shows the result. The particles had a mean size of of app. 150nm, the concentrations in  $D_2O$  were 3.8%, 5.8% and 12% (Fig. 7). For such experiments, we needed app. 3600 to 6000 rocking curves, each of them consisted of app. 300 points (channels), to reconstruct a 2D image of the sample.

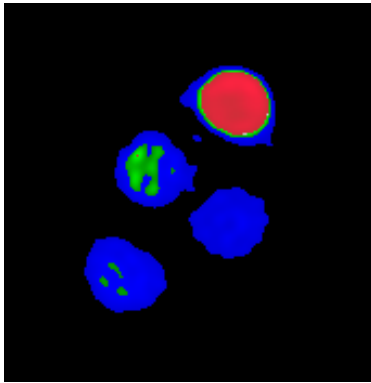


*Fig. 7*

*2D - reconstruction from pure small angle scattering data. Blue = 3.8 % concentration, green = 5.8 % concentration, red = 12% concentration. Note, that the surrounding Al block as indicated in Fig.8 was not reconstructed*

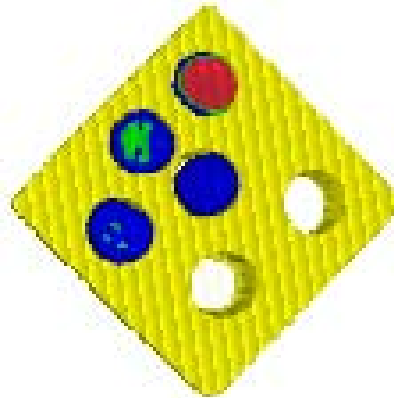


*Fig. 8*

*Combined small angle scattering (colored holes) and Al matrix with several holes. Note that now 6 holes are imaged*

## Summary

We could realise a 2D image reconstruction from pure refraction and from small angle scattering data. Even in the case that no or only very weak absorption is present, we could reconstruct perfect images. Different particle concentrations with a mean size of 150nm could be two-dimensionally resolved. The position resolved small angle scattering might be important if the absolute location of density fluctuations of particles is required. This information is lost in conventional small angle scattering and also cannot be detected with “classical” tomography.

This work was supported by the BMBF project 03TR9B6

## References

- [1] J. Radon, Berichte Sächsischer Akademie der Wissenschaften 29 (1917) 262
- [2] G.T. Herman, Image Reconstruction from Projections, Computer Science and Applied Mathematics, Academic Press, New York, 1980
- [3] Kak, A. C. Slaney, M. (1999) In: *Principles of computerized tomographic imaging*, IEEE, N.Y. p. 49
- [4] Herman, G.T. *Topics in Applied Physics*, Vol. 32, Springer, Berlin, (1979)
- [5] W. Treimer, in *Nuclear Physics*, World Scientific Publishing Co., Proc. XX Brazilian Workshop 1997, p 353 – 363 (1998)
- [5] W. Treimer, U. Feye-Treimer, C. Herzig; Phys. B 241 – 243 (1998) 1197 – 1203
- [6] K.M. Podurets, V.A. Somenkov, S.Sh. Shil'shtein;(1989). Sov. Phys. Tech. Phys. 34, 654-65
- [7] D. Chapman et al.; (1997) Phys. Med. Biol. 42, 2015 – 2025
- [8] Allman, B. E. et al. Nature, 408, 158 (2000)
- [9] W. Treimer, M. Strobl, A. Hilger, C. Seifert, U. Feye-Treimer Appl. Phys. Lett (2003) 83, 2
- [10] J. Kulda, P. Mikula; (1983). J. Appl. Cryst. 16, 498 – 504
- [11] P. Mikula, P. Lukas, F. Eichhorn; (1988) J. Appl. Cryst. 21, 33 - 37